Density Measurements on $C_{12}E_j$ Nonionic Micellar Solutions as a Function of the Head Group Degree of Polymerization ($j = 5-8$)

Marco Maccarini

Department of Physics and Astronomy, Hicks Building, Hounsfield Road, Sheffield, S37 RH, U.K.

Giuseppe Briganti*

INFM, Department of Physics, University "La Sapienza", P.A. Moro 2, 00185 Rome, Italy

Received: July 29, 1999; In Final Form: March 27, 2000

Density measurements have been performed on water solutions of nonionic surfactants oligooxyethylene glycol−monoether ($C_{12}E_j$ with $j = 5, 6, 7, 8$) in a wide range of temperatures and concentrations. The densities of the pure surfactants in their liquid state were measured too. The observed values are almost a linear combination of the densities of an oil and of an oxyethylene (EO) bulk liquid phases. The deviation from ideality reduces as j increases and may be reflects an entropic contribution due to a partial mixing of the oil and EO termination. A temperature (T_{cross}), at which the $C_{12}E_j$ aqueous solution density coincides with the solvent one up to 50 wt % has been found in all the E_j species. The T_{cross} of the different E_j results to be scaling temperatures for the excess density of these surfactants. The sphere-to-rod transition temperatures are scaling temperatures too; thus it is expected that the differences between these two temperatures be constant for each of the E_j species. In the case of $j = 6$, 7, and 8 the values of the sphere-to-rod transition temperatures are known and these differences are all about 20 °C. For $C_{12}E_5$ only rods were experimentally observed and, coherently, the previous consideration led to a sphere-to-rod transition temperature of −7 °C. The difference between the critical and the crossing temperatures is constant too, at about 15 °C for $j < 8$, whereas for $j = 8$ it is 7 °C. In this case the densities of the separated phases, two degrees above the critical temperature, result to be the same, within 10^{-6} g/cm^3. It implies that, when slightly above the critical temperature, $C_{12}E_8$−water solution undergoes phase separate as it was in microgravitational condition. In our analysis, the $C_{12}E_j$ solution is considered a three-component system: the oil core, the bulk water, and the region containing the aggregate interface, a mixture of water molecules, and EO units. Fixing the density of the oil core and of the bulk water phase respectively equal to those of pure dodecane oil and water at the same temperature, we obtain the density and the molar volume of the micellar interface. These data indicate that the amount of water molecules per EO segment decreases with the number of hydrophilic unit and with temperature. The same conclusion follows looking at the temperatures at which the maximum densities as a function of surfactant species and concentrations occur .

1. Introduction

Surfactants are molecules composed by a hydrophilic and a hydrophobic moiety with opposite behavior in aqueous solution: the polar head is soluble in water and the oil tail is not.[1] The presence of this unique duality in a single polymer chain leads to a wide variety of monomeric aggregates with different shapes and sizes. In particular for nonionic surfactant solutions belonging to the family of C_iE_j (oligooxyethylene glycols), as the temperature increases above a value indicated as the sphere-to-rod transition temperature, the aggregates in solutions turn from spherical shape into elongated cylinders, and at higher temperature phase separation occurs. At high concentration and low temperature many characteristic liquid crystal phases are present.[2−4]

The possible aggregation states of these nonionic surfactants are all characterized by an oil core that maintains a stable composition because of its hydrophobicity. Therefore, its thermodynamic state depends mainly on the local curvature and on the osmotic pressure at its interface. On the contrary, the hydrophilic interface defines a thick region with a wide degree of variability. Within few K_BT of difference there exists many possible states for the local hydration, that is, the number of solvent and eventually cosolvent molecules at the interface, as well as the conformation of the hydrophilic chain, i.e., the interfacial thickness.[2,3,5,6] Hence, this hydrophilic thick interface can adapt its thermodynamic state to solubilize at best the micellar aggregates, with an effectiveness which raises with the size of the hydrophilic moiety.

From an experimental point of view this hypothesis seems to be trusty. In fact the sphere-to-rod transition temperatures observed experimentally in the case of the family $C_{12}E_j$ increases in accordance with the number of EO units per monomer. These temperatures are determined with about 10 °C of variation, depending on different techniques, and result to be 50 °C for $j = 8$, 35 °C for $j = 7$, and 15 °C for $j = 6$; below $j = 6$ only rods are observed above the freezing temperature.[7−10] Therefore, when EO units are added, the stability of spherical aggregate increases.

* To whom correspondence should be addressed.

10.1021/jp992686r CCC: $19.00
Published on Web 11/10/2000

On further increasing the temperature, these solutions part in two phases, one rich and one poor in surfactants.[2,3] Theoretically, dehydration, or more generally the EO−solvent composition at the micellar interface,[6,10] is also considered the driving mechanism for the phase separations in the C_iE_j−water solutions[11,12] as well as in the EO−water solutions.[13,14] The interaggregate London force increases with temperature, but not enough to justify the observed critical temperatures, and therefore hydration forces are needed to drive these phase separations.[1] Again, the interfacial polymer conformation and the local composition can play the main role in determining the strength of the hydration forces. The critical temperatures of these upward curves of coexistent phases increase with the number of hydrophilic terminations *j*. Hence the isotropic phases of these micellar solutions enlarge their extent in the phase diagrams on increasing the molar volume of the monomeric hydrophilic side.

The previous considerations lead to two conclusions. First, the micellar solutions are constituted by three regions in equilibrium: the bulk solvent phase and the two micellar subregions, the oil core, and the interfacial EO−water mixture. Second, the interfacial EO−water solution properties, conformation and composition, play the main role in stabilizing the overall thermodynamic state of these nonionic micellar solutions.

A detailed analysis of the interfacial polymer−solvent region is thus needed for a satisfactory understanding of the complex thermodynamic behavior concerning these systems. The theoretical description of the interfacial micellar region is generally poor. A very detailed and highly successful model for micellar formation in the case of the C_iE_j surfactants has depicted the anchored hydrophilic heads such as an effective hard disk.[6] It means that the headgroup conformation and the local interfacial composition are described as an excluded cross-sectional area per monomer at the micellar interface. In this theory the value of the hard disk cross sectional area increases with *j* and contributes to predict the cmc (critical micellar concentration) and the sphere-to-rod transition temperatures for all the C_iE_j surfactants.

The free energy difference between trans and the gauche isomeric rotational states was used to build up a thermodynamic model for the hydrophilic chain conformations at the micellar interface. This model predicts a very wide variety of possible polymer conformations, which depend on temperature and on the number of E_j segments.[15] In this model, the interfacial local composition is considered as an effective interaction potential for the polymer segments.

The theories concerning anchored polymer suppose the system incompressible and these models give analytical results only at high degrees of polymerization and at low surface density; for short chains only numerical results are available.[16] Numerical evaluations of the polymer conformations were performed on the basis of the RIS model (rotational isomeric state) at a low degree of polymerization.[17] The results indicate that, in water solution, the end-to-end distance of the polymer chain fulfills the scaling law within 2% error in free EO chains possessing 12 bonds. For anchored EO the same error is obtained with 30 bonds. Thus, for degrees of polymerization between 5 and 8 (from 15 to 24 bounds) as is the case of our samples, scaling laws are not helpful for the determination of the interfacial thickness. Hence neither the interfacial composition nor the interfacial thickness can be inferred from any theoretical approach.

On the other hand, interesting new information on these solutions can be obtained using any experimental techniques able to contrast the interfacial region respect to the oil core and the bulk water. This kind of experiments can give numerical evaluations of the physical properties concerning each of the micellar regions and, in particular, of the interfacial one. Density measurements belong to this category since the local density is related to the local composition through the mass of the components present in any defined region. We witness that this technique produces a satisfactory contrast among the water phase, the oil core, and the interface micellar regions. In fact, using as reference for the density of these regions that of the relative bulk phases, it comes out that the oil bulk phase, reference for the oil core, has a density of $\sim$0.75 g/cm^3, the water density is $\sim$1.00 g/cm^3, whereas the density of EO-water mixtures, used as reference for the interfacial region, ranges between 1.00 and 1.10 g/cm^3 at 25 °C.

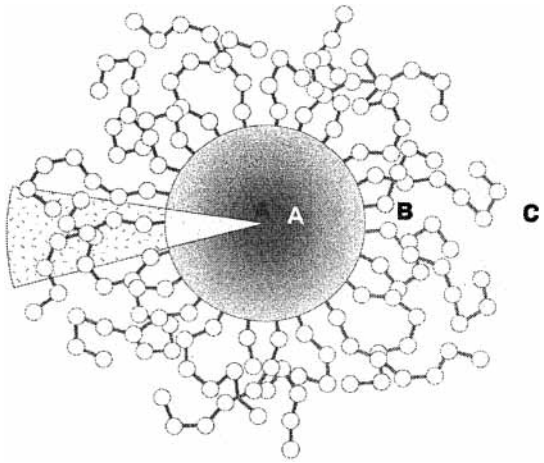

Figure 1. Schematic view of a cross section of a micellar aggregate (spherical or cylindrical). The area named A represents the oil core region, B the interfacial region with EO terminations and water, C the bulk water phase. The volume indicated on the left side represents the hydrated volume per monomer, divided in its parts: head and tail; the rectangle at the top schematize the interfacial EO−water mixture.

2. Material and Methods

The samples analyzed ($C_{12}E_5$, $C_{12}E_6$, $C_{12}E_7$, $C_{12}E_8$) were purchased from Nikko Chemicals and were diluted without any further purification. The concentration of the different water solutions was established by weighing the components. Density measurements were performed with Paar digital density meter DMA60 combined with the remote cell DMA 602, which can provide an accuracy up to $\pm 1.5 \times 10^{-6}$ g/cm^3, according to the oscillating sample tube method. The external cell was thermostated by Heto DBT6 thermostat and Heto CB8-30e cooling bath which guarantees a temperature stability within 0.05 °C. The Paar instrument we used does not compensate for viscosity. On increasing the sample viscosity, the interface between the tube and the liquid surface induces an extra resonance. As a result, the overall resonance of the tube (that depends on the solution density) is shifted. At the highest concentrations of our solutions, the experimental viscosity[18] reduces the accuracy of our measurements to $\pm 1 \times 10^{-4}$ g/cm^3.[19]

3. Data Analysis

In Figure 1 a schematic view of the cross section of a spherical or cylindrical micelle is reported. In our model of nonionic micellar solution the oil core volume (*A*) is obtained from the bulk oil phase density. The molar volume of the bulk

water (*C*) is known. On the other hand, the interfacial volume of the headgroup termination (*B*) can greatly vary. Depending on the polymer's conformation, the polymer molarity in the (*B*) region changes and different amounts of water are needed to fill it up to the correct density. Thus these solutions can be considered as a tricomponent and we make the hypothesis that the three regions have a well-defined thermodynamic average; i.e., a reliable value of the relative densities.[20] This could not be the case for a single micelle or for a free monomer but, since density measurements represent an average over a wide number of aggregates and monomers in solution, we are allowed to define, in the thermodynamic limit, an average value for the oil core density and one for the interfacial region, which depend on the average aggregate shape and size. The volume of a solution of n_w moles of water and n_s moles of surfactant can generally be written as

$$V = n_w \tilde{V}_w^0 + n_s \phi_v \tag{1}$$

where $\tilde{V}_w^0$ is the molar volume of bulk water and ϕ_v the apparent molar volume of the surfactants. The molar volume of the solutions is then given by

$$\tilde{V} = (1 - x_s)\tilde{V}_w^0 + x_s \phi_v \tag{2}$$

In the framework of our picture we assume the following:

(i) the monomer contribution is negligible since our concentrations are much larger, above 1 mM, than the cmc concentrations of these surfactants;

(ii) each surfactant molecule in the average aggregate is hydrated, the hydration water molecules are mainly located in the outer shell of the micelle, and, in general, their molar volume $\tilde{V}_w^h$ is different from that of the bulk water $\tilde{V}_w^0$;

(iii) the hydrated volume of the surfactant is given by $V_s^h = \tilde{V}_s + N_w^h V_w^h$, where N_w^h is the number of hydration water molecules per surfactant and V_s the unhydrous monomeric volume of the surfactant.

According to these assumptions, we consider the solution as an "ideal" binary mixture of $N_w - N_w^h N_s$ water molecules and N_s molecules of hydrated surfactants:

$$V = (N_w - N_w^h N_s)V_w^0 + N_s V_s^h = N_w V_w^0 + N_s[\tilde{V}_s - N_w^h(V_w^h - V_w^0)] \tag{3}$$

Combining eqs 1 and 3 we obtain the following equation for the apparent molar volume:

$$\tilde{\Phi}_v = \tilde{V}_s^h - N_w^h \tilde{V}_w^0 = \tilde{V}_s\left(1 + N_w^h \frac{\tilde{V}_w^h - \tilde{V}_w^0}{\tilde{V}_s}\right) \tag{4}$$

Since $\tilde{V}_w^h - \tilde{V}_w^0$ is of the order of the unit and $\tilde{V}_s$ can vary from 700 to 1000 Å^3, the correction to the unhydrous monomeric volume is negligible. Then the experimental apparent molar volume of the solution corresponds to the unhydrous volume of a surfactant within the average micellar aggregate. From this evaluation we can obtain the anhydrous volume of the polar head:

$$\tilde{V}_h = \tilde{V}_s - \tilde{V}_t \tag{5}$$

since $\tilde{V}_t$, in our analysis, is equal to the dodecane oil molar volume. On the same basis, the solution density is then given by

$$\rho = \frac{\tilde{M}}{\tilde{V}} = \frac{(1 - x_s)M_w + x_s M_s}{\tilde{V}}(1 - \phi_s)\rho_w + \phi_s \rho_s \tag{6}$$

where M_w and M_s are the molecular weights of water and of the surfactant, respectively, ϕ_s is the surfactant hydrated volume fraction, and ρ_s represents the density of a hydrated monomer in the average micellar aggregate. So, if we define ρ_h, $1 - \phi_t$ and ρ_t, ϕ_t the density and the volume fraction respectively of the interface and of the oil core within the average micellar aggregate, we can write

$$\rho_s = \phi_t \rho_t + (1 - \phi_t)\rho_h \tag{7}$$

Furthermore, at a constant number of particles N_s and N_w, we have[20]

$$\rho_w = \frac{M_w}{\tilde{V}_w} \quad \rho_s = \frac{M_s + N_w^h M_w}{\tilde{V}_s^h} \tag{8}$$

$$\phi_w = \frac{(N_w - N_w^h N_s)V_w}{V} \quad \phi_s = \frac{N_s V_s^h}{V} \tag{9}$$

Combining eq 6 and 7 with the above definitions (eqs 8 and 9), ρ_h is given by

$$\rho_h = \rho + \frac{1}{V_h^h}\left[V_t(\rho - \rho_t) + \frac{N_w - N_w^h N_s}{N_s} V_w(\rho - \rho_w)\right] \tag{10}$$

where V_h^h is the hydrated average volume per monomer of the polar head at the micellar interface. This volume represents the frustum of cone that extends as far as the end-to-end distance of the hydrophilic EO termination, from the micellar oil core interface up to the bulk water phase. It is different from the unhydrous volume obtained in eq 5 since it contains some amount of water, i.e., the hydration water molecules. To get rid of the dependence from the unknown N_w^h variable in ρ_h, we use the condition for the interfacial density:

$$\rho_h = \frac{M_h + N_w^h M_w}{V_h^h} \tag{11}$$

where M_h is the molecular weight of the head termination, we can finally give the following equation for the density ρ_h inside the volume V_h^h:

$$\rho_h = \frac{\rho_w}{\rho}\left\{\rho + \frac{1}{V_h^h}\left[V_t(\rho - \rho_t) + \left(\frac{1 - x_s}{x_s} + \frac{M_h}{M_w}\right)V_w(\rho - \rho_w)\right]\right\} \tag{12}$$

where x_s is the surfactant mole fraction. The evaluation of the densities of the C_iE_j aggregates in water solutions depends on the hydrated volume per monomer V_h^h at the micellar interface. No univocal indication can be obtained about this volume from scattering experiments, since its evaluation depends on the specific contrast each of these techniques has of the interfacial region.[7,21] Therefore, in our analysis, we extract the interfacial density from that of the $C_{12}E_j$ solutions as a function of the parameter V_h^h and of the temperature. These equations will be used in the following experimental analysis. It has to be noted that, whereas density is taken as a parametric function of the hydrated monomer volume, the anhydrous partial molar volume

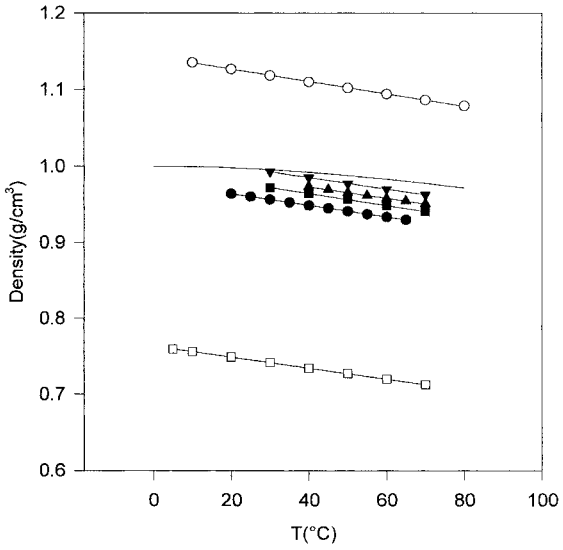

Figure 2. Density of EO polymer PEG600 in its liquid state (open circles), of pure $C_{12}E_5$ (filled circles), $C_{12}E_6$ (filled squares), $C_{12}E_7$ (filled triangles up), $C_{12}E_8$ (filled triangles down) liquid surfactant, of water (full line), and of dodecane (open square).

of the EO terminations at the micellar interface is univocally determined from the experimental data.

4. Experimental Results for Pure Surfactants

First we analyze the density of the pure surfactants in their liquid state. The liquid phases of a pure surfactant $C_{12}E_j$ is, in our model, a two-component system: there is no water; in this case the density is simply given by eq 7.

The densities of the pure samples versus the temperature are plotted in Figure 2. For comparative purpose the pure PEG600,[22] the water and the bulk dodecane densities are reported too. It has to be noted that polymer solutions at intermediate and high concentrations possess thermodynamic properties which do not depend on the degree of polymerization.[23] Then the comparison of the PEG600 solution density, which has 13 EO units, with the interfacial solution density, containing 5, 6, 7, and 8 EO units, is consistent only if the EO concentrations are above 4−5 molar.

The observed values for the different $C_{12}E_j$ are between the oil and the EO density; $C_{12}E_8$ is closer to the EO whereas $C_{12}E_5$ has a lower density closer to that of the oil phase; i.e., increasing the EO units the surfactant density results closer to the pure EO polymer density. Thus, at first, we tried to calculate the density of the liquid surfactant as an ideal combination of the bulk oil and EO density, weighed by the relative volume fraction. The comparison of the obtained ideal densities (ρ^{id}_{pure}) with the experimental value (ρ^{ex}_{pure}) shows a systematic discrepancy, constant with temperature and equivalent for all the $C_{12}E_j$ species.

To take it into account, we assume the presence of an intermediate region where the head and the tail terminations are mixed together. Therefore, there will be three regions: an oily region with a density equal to the bulk dodecane, a polar region with a density equal to the pure EO, and an intermediate region between the former two. In the pure surfactant liquid phase, even though we cannot talk of any aggregation state, monomers organized in sequence of hydrophilic and hydrophobic regions optimize the free energy of the system. This simply reflects the fact that the intermonomer interaction favors (EO−EO) and (oil−oil) rather than (EO−oil) interactions. For $T = 0$ K this would imply a complete segregation of oil and EO in different regions. In our temperature range (5−70 °C), entropic competition causes a partial mixing of these two regions. We thus obtain the following expression for the density of the pure surfactant:

$$\rho = \phi_h\rho_h + \phi_t\rho_t + \phi^*\rho^* \tag{13}$$

where ϕ^* and ρ^* indicate the volume fraction and the density of the intermediate region. On the other hand

$$\rho^* = \frac{\tilde{M}^*}{\tilde{V}^*} = \frac{mM_{EO} + nM_{CH_2}}{\tilde{V}^*} \tag{14}$$

$$\tilde{V}^* = \tilde{V}_s - (\tilde{V}_h + \tilde{V}_t) = \frac{M_s}{\rho} - \left[(j-m)\frac{M_{EO}}{\rho_h} + (i-n-1)\frac{M_{CH_2} + M_{CH_3}}{\rho_t}\right] \tag{15}$$

where M_{EO} and M_{CH_2} are the molecular weight of an EO monomer unit (CH_2-O-CH_2) and of a CH_2; n and m are the number of CH_2 and EO in the intermediate region. It is then possible to obtain an explicit expression for ρ^* that depends on the number m and n of EO and CH_2 groups included in this intermediate region:

$$\rho^* = \frac{nM_{CH_2} + mM_{EO}}{\left(\frac{M_s}{\rho} - \frac{(j-m)M_{EO}}{\rho_h} - \frac{(11-n)M_{CH_2} + M_{CH_3}}{\rho_t}\right)} \tag{16}$$

By including or excluding EO and CH_2 groups from the intermediate region, we will get different values of ρ^*. The correct one should have an intermediate value between ρ_h and ρ_t such that the theoretical density, evaluated with eq 13, results to be equal to the experimental one.

We can thus obtain the minimum number for n and m included in the intermediate region that gives the experimental density. In all our samples these numbers are two CH_2 from the tail and two CH_2-O-CH_2 from the head, i.e., $n = m = 2$ in eq 13. The results show that ρ^* does not depend on the degree of polymerization of the polar head. It means that in order to obtain the density of pure $C_{12}E_{j+i}$ we can simply sum the contribution due to the i added EO group at the value of the density of pure $C_{12}E_j$, considering them part of the pure EO region. Within a few percent the values of $C_{12}E_{j+i}$ obtained coincide with the experimental one for all i and j combinations between 5 and 8.

As a conclusion we can say that surfactants' liquid phases possess densities which are the ideal combination of the oil density, the EO density, and the density of two CH_2 and two EO, characterizing an intermediate region, weighed with their relative volume fractions. The definition of the intermediate region could be affected by samples not completely dehydrated since $C_{12}E_j$ is strongly hygroscopic. But an error in the surfactant concentration, i.e., in the amount water in the sample, could only affect the numerical determination of n and m in our analysis.

An important hypothesis regarding the $C_{12}E_j$−water solutions can be stated from the previous considerations: we saw that the density of the hydrophobic region can be considered equal to the corresponding bulk oil. The interfacial region can change conformation and the number of adsorbed solvent molecules; this can stabilize the oil core against the bulk water phase by

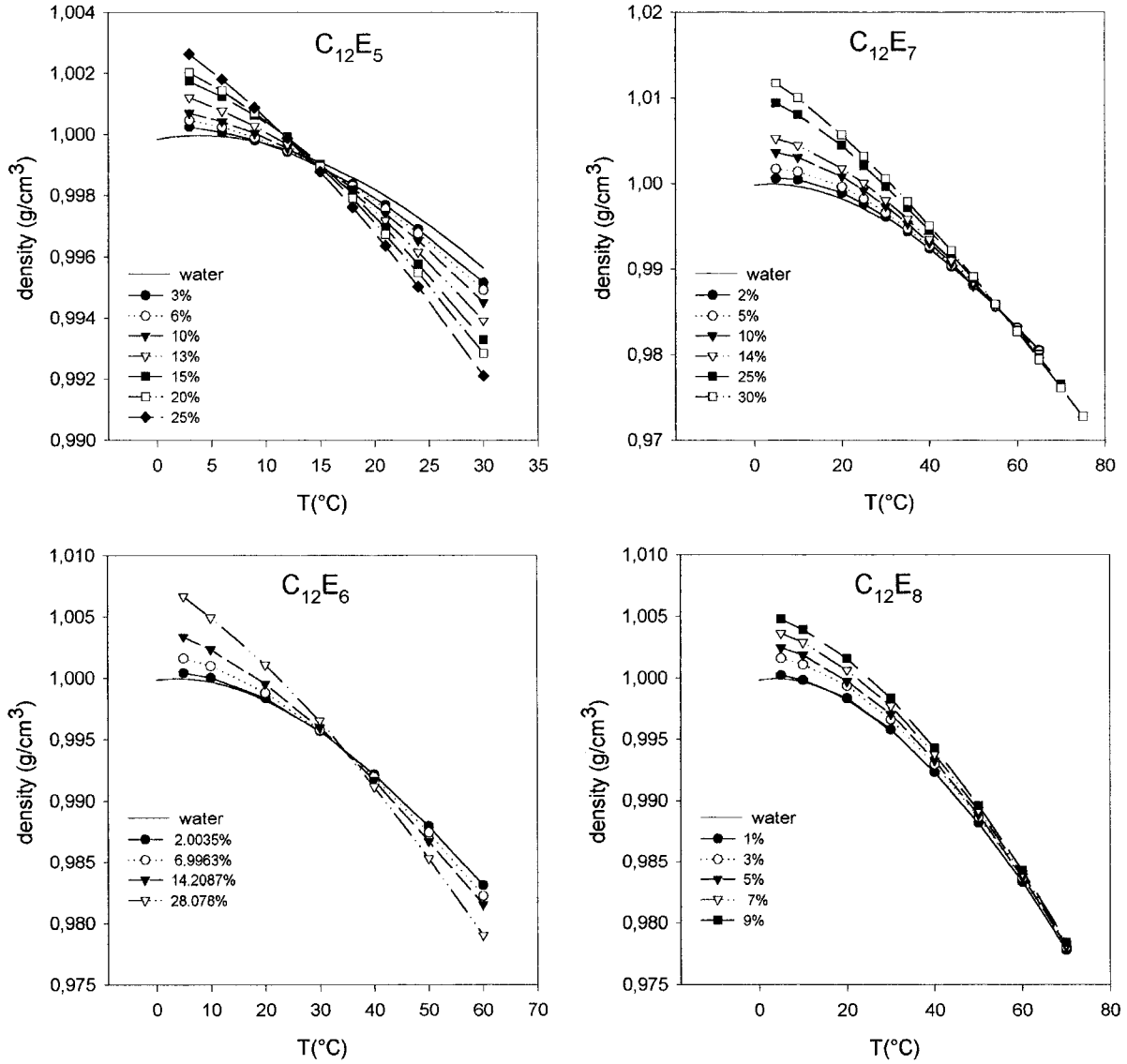

Figure 3. Density of solutions of water and $C_{12}E_j$ with $j = 5, 6, 7, 8$ are reported as a function of the temperature, for different concentrations. For comparison the water density (continuous line) is reported too.

taking advantage of these degree of freedom. Thus, in all the following analysis the density of the micellar core will be taken equal to the one of the bulk dodecane.

5. Experimental Results for Surfactant in Solutions

The experimental densities, as a function of temperature and at different surfactant concentration, are reported in Figure 3a,b,c,d for j going from 5 to 8, respectively. At first glance, it is evident the presence of a crossing temperature T_{cross} at which the solution density coincides with the solvent one up to 50% surfactant concentration by weight. In all our samples the density decreases with temperature; when $T \leq T_{cross}$ the density of the solution is higher than that of water and the opposite happens when $T \geq T_{cross}$. In these nonionic surfactant solutions it was generally observed that, after phase separation, the phase at lower concentration has a higher density and lies at the bottom of the sample holder. The surfactant-rich phase is on the top, being lower in density.[24] Thus, at least for all these samples, T_{cross} must be lower than the critical temperature.

Solutes in water have been phenomenologically divided into *structure former* and *structure breaker* if the maximum of the solution density moves at a lower or higher temperature, respectively.[25] With a quadratic fit of the experimental curves, we evaluated, for each surfactant concentration, the temperature at which the density reaches its maximum value. In Figure 4 the values of RT_{max} are reported as a function of the surfactant mole fraction for the different E_j species. A linear trend with a negative slope is observed for all of them, indicating that our samples are structure formers. It has to be noted that in the limit of zero surfactant concentration all the intercepts give for RT_{max}, the value obtained in pure water within a 5% range of error.

The slopes of these lines, related to the surfactant structure former attitude, are a measure of the change in the solvent hydrogen-bound network due to the solubilization of a monomer within an aggregate. The experimental slopes, reported in the inset of Figure 4, are between 1 and 4 times the hydrogen bond energy. It is evident that on increasing the EO units per monomer, the structuring effect of the surfactant reduces. The monomer−water interaction is mainly confined in the interfacial region, and thus this result indicates that the EO exposure to the solvent decreases as the monomeric degree of polymerization rises. Furthermore, the values of the slope as a function of j show an alternating behavior around a best fit curve; for even j it is higher than the fitting values and it is lower for odd j.

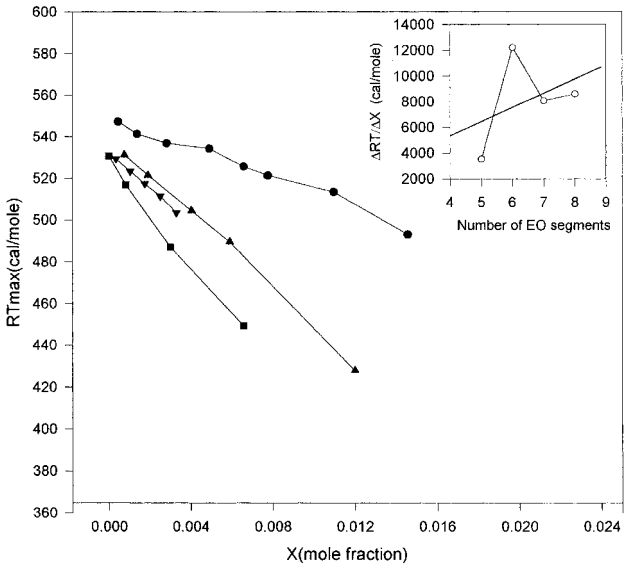

Figure 4. Values of RT_{max} as a function of the surfactant mole fraction for $C_{12}E_5$ (full circles), $C_{12}E_6$ (full squares), $C_{12}E_7$ (full triangles up), and $C_{12}E_8$ (full triangles down). A linear trend with a negative slope is observed for all the E_j species. The slopes of these lines are reported in the inset.

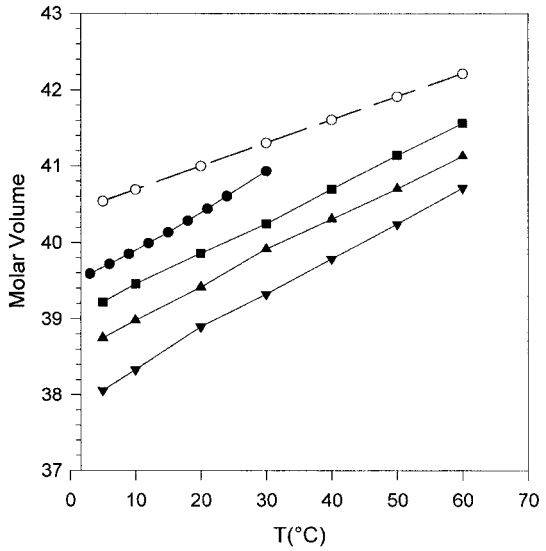

Figure 5. Molar volume per EO units at the micellar interface for $C_{12}E_5$ (full circles), $C_{12}E_6$ (full squares), $C_{12}E_7$ (full triangles up), and $C_{12}E_8$ (full triangles down) plotted as a function of the temperature; the molar volume per EO units in a solution of water and PEG600 (open circles) is reported too.

Such even/odd alternating behavior was observed in the adsorption properties of *n*-alkyloligooxypropylene ether too and represents still an open problem for these solutions.[26]

From the apparent molar volumes of our samples we evaluate, using eq 5, the dry molar volume of the polar heads. Dividing these values by the degree of polymerization of the relative surfactant species, we obtained the dry molar volume per EO unit for the different surfactants ($V_h(j)/j$). In Figure 5 we report our results, the molar volume per EO units for a solution of water and PEG600[22] is reported too. In all the cases a linear trend with temperature is observed. The EO molar volume of $C_{12}E_5$ is closer to the one of the EO−water solutions and in $C_{12}E_6$, $C_{12}E_7$, and $C_{12}E_8$ it decreases progressively. Also this result reinforces the hypothesis of a reduction of the EO exposure to the solvent with *j*. Thus in the hydrated average

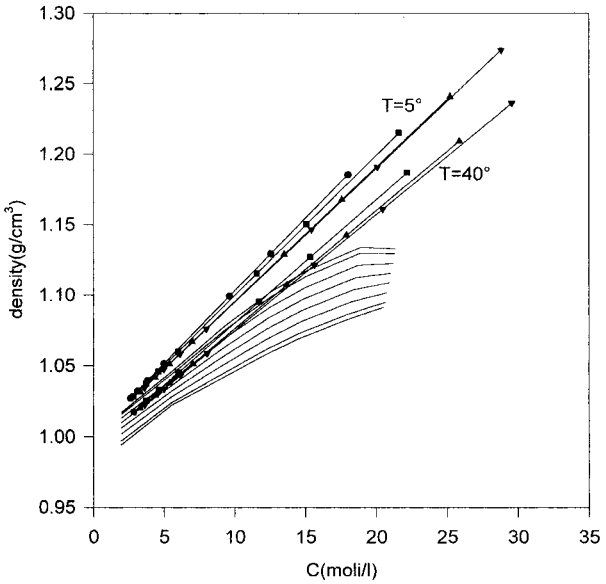

Figure 6. Value of ρ_h as a function of the EO molarity at the micellar interface ($j/V_h^h(j)$) reported for $C_{12}E_5$ (full circles), $C_{12}E_6$ (full squares), $C_{12}E_7$ (full triangles up), and $C_{12}E_8$ (full triangles down) at two temperatures, 5 and 40 °C. The density data of EO−water solutions as a function of EO molarity and for different temperatures, from 5 to 45 °C, are reported too.

volume per monomer, V_h^h defined after eq 10, the portion occupied by each of the EO unit decreases going from $j = 5$ to $j = 8$. Furthermore, it indicates that the overall interfacial density is characterized by a higher contribution from the EO units than in EO−water solution at the same temperature and concentration.

The values of ρ_h obtained by using eq 12 at a fixed temperature and surfactant concentration, depend on $1/V_h^h$. Since *j* is fixed for each surfactant species, this equation defines the values of ρ_h as a function of the EO molarity at the micellar interface. In Figure 6 these trends for ($C_{12}E_5$, $C_{12}E_6$, $C_{12}E_7$, $C_{12}E_8$) are reported at two different temperatures, 5 and 45 °C. The densities of EO−water solutions as a function of EO unit molarity and for the different temperatures, from 5 to 45 °C, are also reported. As suggested by the considerations made on the EO molar volume, the interfacial densities of all the E_j species are higher than that of the EO polymer in water solutions at the same temperature. However, the interfacial density of $C_{12}E_8$ is lower than the one of $C_{12}E_5$ and closer to the density of the EO−water solutions at the same temperature. On combining this with the increase of the partial molar volume of EO units with *j*, the number or the density of the interfacial water molecules per EO unit must decrease with *j*; i.e., each EO unit in $C_{12}E_8$ is less hydrated than those in $C_{12}E_5$. From our results we cannot univocally determine either the end-to-end distance of the EO termination or the volume V_h^h; thus the cross-sectional area per polar head cannot be evaluated. Nevertheless, the observed reduction of the degree of hydration with increasing *j* suggests that the hydrophobic oil−water repulsion decreases at the oil−core interface. As a consequence, the cross-sectional area per chain termination can increase with *j*, and this consideration agrees with those obtained from surface tension measurements in nonionic surfactants.[27]

As a conclusion to this section, we present the excess density computed from the experimental results on two different thermodynamic representations. The first, used for symmetric solutions, defines the reference state as an ideal combination of the density of the pure components: water and surfactant.

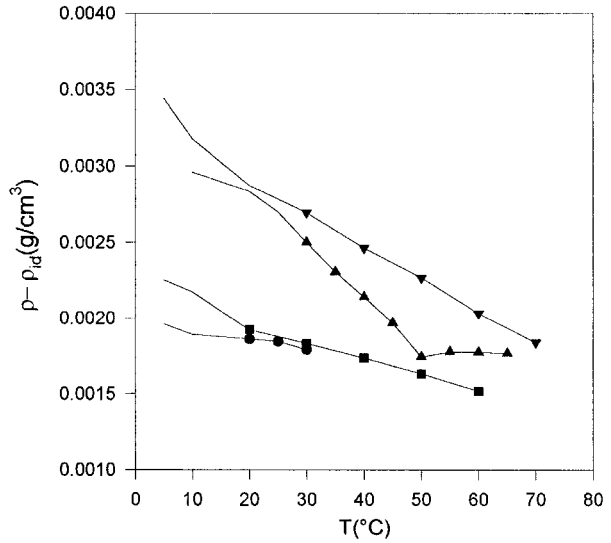

Figure 7. Excess ideal density for solutions of water and $C_{12}E_5$ (full circles), $C_{12}E_6$ (full squares), $C_{12}E_7$ (full triangls up), and $C_{12}E_8$ (full triangles down). The values are obtained from the data at a low surfactant concentration; at the temperature below the pure surfactant freezing point the density of the pure surfactant was evaluated by extrapolation from the liquid phase.

The second, used for diluted solutions, has the solvent density as its reference state.[20] In the former case the excess density is given by

$$\rho_{\text{excess}} = \rho_{\text{measured}} - \rho_{\text{ideal}} \tag{17}$$

with

$$\rho_{\text{ideal}} = (1 - \phi_s^a)\rho_{\text{water}} + \phi_s^a \rho_{\text{pure surfactant}} \tag{18}$$

where ϕ_s^a is the volume fraction of the anhydrous surfactant. In Figure 7 the excess ideal density is reported for all the different monomeric species. The values are taken from data obtained at a low surfactant concentration. At temperatures below the pure surfactant freezing temperature, the densities of the pure surfactants were extrapolated from the temperature dependence of the relative liquid phases.

For $C_{12}E_7$ the excess ideal density presents a breaking temperature at 45 °C, between the sphere to rod transition and the crossing temperatures. In the case of $C_{12}E_5$ and $C_{12}E_6$ the sphere to rod transition temperature is below the pure surfactant freezing temperature, whereas for $C_{12}E_8$ it is too close to the demixing temperature; thus in these other cases any breaking temperature cannot be reliable. But in any case it is evident that in those nonionic surfactant solutions the micellar interfacial region undergoes many structural rearrangements on increasing temperature.

In the framework of dilute solutions[20] the excess density is given by

$$\rho_{\text{excess}} = \rho_{\text{measured}} - \rho_{\text{water}} \tag{19}$$

For this case the results are shown in Figure 8a, where the data are normalized on the concentration. In Figure 8b the same graph of Figure 8a is given as a function of $T - T_{\text{cross}}$; with this abscissa scale the dilute excess densities of the different surfactant monomers rescale one over the other; then T_{cross} represents a scaling temperature for them. The sphere to rod transition temperature, T_{sr}, is a scaling temperature too, and in fact the difference between T_{cross} and T_{sr} is a constant, about 20 °C, in $C_{12}E_6$, $C_{12}E_7$, and $C_{12}E_8$, where the sphere to rod transition temperatures are known. In $C_{12}E_5$ spherical aggregates were never observed and, consequently, the previous consideration gives in this case $T_{\text{sr}} = -7$ °C.

6. Discussion and Conclusions

The experimental results on each of the pure surfactant species, in their liquid states, unambiguously indicate that most of the oil and EO terminations possess values of density equivalent to those of the bulk respective phase. In all the investigated surfactant species there exists an equivalent intermediate region containing two CH_2, and two CH_2-O-CH_2 units. The existence of this region is, in our opinion, due to the entropy of mixing of the surfactant monomers at their bonding.

Micellar aggregates in water could present features similar to that of the pure surfactant one: an intermediate region could exist at the bonding between the hydrophilic and hydrophobic moieties, where water molecules as well as hydrophobic and hydrophilic units are present. This region could correspond to the theoretically predicted roughness at the micellar interface.[28,29] Following the hypothesis made for the pure surfactants, the oil core must have a density equal to the one of an oily bulk phase,

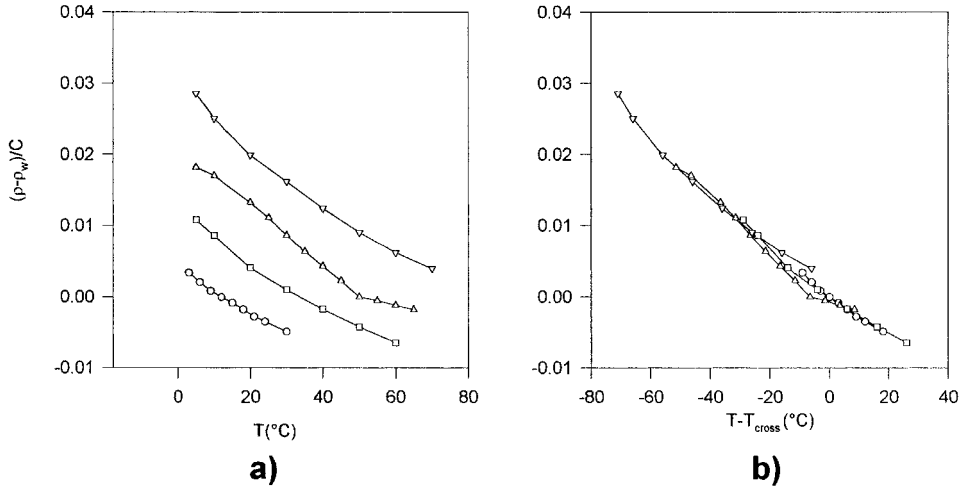

Figure 8. (a) Excess diluted solution densities, normalized on solution concentrations, for the solution of water and $C_{12}E_5$ (full circles), $C_{12}E_6$ (full squares), $C_{12}E_7$ (full triangles up), and $C_{12}E_8$ (full triangles down) as a function of the temperature. (b) The same quantities are plotted as a function of $T - T_{\text{cross}}$. With this abscissa scale the normalized excess diluted solution densities of the different surfactant monomers rescale one over the other.

whereas the outer interfacial EO−water mixture must correspond to an equimolar EO−water solution at the same temperature. The intermediate region can have an arbitrary density between the one of the oil and the one of the outer EO−water mixtures. This point of view was already proposed by one of the authors analyzing static dielectric measurements in $C_{12}E_6$ and $C_{12}E_8$ solutions as a function of temperature. This data indicates that the EO molarity at the interface ($j/V_h^h(j)$) increases with temperature and number of j terminations. In the case of $C_{12}E_8$ the interfacial molarity reaches, at high temperatures, values close to that of the pure EO polymer in its liquid phase.[30] Somehow, highly dense polymers anchored onto an interface could have a sort of brush to mushroom transition at a low degree of polymerization due to the interpolymer interaction. In the mushroom configuration the outer EO−water mixture, the hat of the mushroom, can reach compositions highly concentrated in EO terminations, close to the value observed with dielectric spectroscopy. The density we obtain from eq 12 is only an average density over the entire volume of the head termination (V_h^h) and an intermediate region cannot be distinguished. Therefore, the above picture of the interfacial region can be verified only through a comparative analysis of these data with other complementary experimental techniques.

In any case, our results suggest that with the degree of polymerization, j, the number of water molecules enclosed in the interfacial region decreases, supporting an increase of the EO molarity. Indeed, the molar volume per EO unit in the polar interface ($V_h(j)/j$) decreases with the number j of EO terminations per monomer. Thus the contributions to the interfacial density due to the EO termination $(\tilde{M}/\tilde{V})_{EO}$ increase with j. Since experimentally we observed a decrease with j of the interfacial density, we must conclude that the degree of hydration per EO unit decreases with j.

The same considerations can be stated looking at the values of the maximum in density at different surfactant concentrations and for different surfactant species. The inset of Figure 4 shows that the increase of the hydrogen-bound network saturates increasing the number of j terminations per monomer, i.e., the EO−water interfacial mixture decreases its water content with j.

On increasing the temperature, each of the surfactant species dehydrates, correspondingly the EO partial molar volume increases with the temperature, and its contribution to the interfacial density decreases. However, the experimental interfacial density decreases more than the partial molar volume of the EO units can induce; that means dehydration is needed to fulfill the experimental results in this case too.

For all the surfactants the interfacial density from eq 6 results to be bigger than any EO−water solutions at the same temperature (see Figure 6). This excess contribution must be due to the confinement of the surfactant monomer into the aggregate which depends on temperature and number of j terminations.

Some further considerations have to be devoted to the observed scaling properties. It is generally known that the micelle undergoes structural rearrangements at different temperatures depending on the number of EO units per surfactant monomer. The sphere to rod transition and the crossing temperatures are peculiar to each of the investigated surfactant species. Their relative differences do not depend on the monomeric degree of polymerization and it results to be about 20 °C.

The critical temperatures of all the measured surfactant species are higher than the experimental crossing temperatures, and therefore the surfactant-rich phase floats above the water-rich phase after demixing under the gravitational gradient. The difference between the crossing and the critical temperatures is nearly constant (15 ± 0.5 °C) for $j = 5$, 6, and 7, whereas it is about 7 °C for $j = 8$. Extrapolating our results to some temperature, above the critical temperature, we can determine the density of the two phases after separation. In fact, if the tie lines connecting the separated phases are horizontal, it is easy to get from the phase diagram the concentrations of each of the surfactant solutions after the mixing. At 1 °C above the critical temperature, for all the surfactant species with $j < 8$, the concentrations of the two phases are 1.5 and 25 wt % (wt % is the percentage in weight) the relative densities are 0.983 and 0.977 g/cm^3 and a slow demixing can occur under a gravitational field. In the case of $C_{12}E_8$ the crossing temperature and the critical temperature are closer, 7 °C difference, and the temperature derivative of the density is nearly constant with concentration. It then follows that the densities of the two separated phases are the same within 10^{-6} g/cm^3 difference up to 2 deg above the critical temperature. Thus in the case of $C_{12}E_8$ the phase separation occurs under a sort of microgravitational field.

Acknowledgment. The authors thank Prof. Giovanni D'Arrigo for his useful suggestions on the molar volume analysis as well as Prof. Giovanni Ciccotti for his comments on the first writing of this work. This work was supported by INFM and ASI.

References and Notes

(1) Israelachvili, J. N. *Intermolecular and Surface Forces*; Academic Press: London, 1985; Chapter 15.
(2) Nilsson, P. G.; Wennerstrom, H.; Lindman, B. *J. Phys. Chem.* **1983**, *87*, 1377.
(3) Kahlweit, M.; Strey, R.; Haasse, D. *J. Phys. Chem.* **1985**, *89*, 163.
(4) Mitchell, D. J.; Tiddy, G. J. T.; Waring, L.; Bostock, T.; MacDonald, M. P. *J. Chem. Soc., Faraday Trans. 1* **1983**, *79*, 975.
(5) Briganti, G.; Bonincontro, A. *Colloids Surf.* **1998**, *140*, 313.
(6) Puvvada, S.; Blankshtein, D. *J. Chem. Phys.* **1990**, *92*, 3710.
(7) Zulauf, M.; Weckstrom, K.; Hayter, J. B.; Degiorgio, V.; Corti, M. *J. Phys. Chem.* **1985**, *89*, 3411.
(8) Kato, T.; Anzai, S.; Seimiya, T. *J. Phys. Chem.* **1990**, *94*, 7255.
(9) Corti, M.; Degiorgio, V. *J. Phys. Chem.* **1981**, *85*, 1442.
(10) Briganti, G.; Puvvada, S.; Blankschtein, D. *J. Phys. Chem.* **1991**, *95*, 8989.
(11) Kjellander, R. *J. Chem. Soc., Faraday Trans. 2* **1982**, *78*, 2025.
(12) Karlstrom, G.; Carlssons, A.; Lindman, B. *J. Phys. Chem.* **1990**, *94*, 5005.
(13) Kjellander, R.; Florin, E. *J. Chem. Soc., Faraday Trans. 1* **1981**, *77*, 2053.
(14) Karlstrom, G. *J. Phys. Chem.* **1985**, *89*, 4262.
(15) Bjorling, M.; Linse, P.; Karlstrom, G. *J. Phys. Chem.* **1990**, *94*, 471.
(16) Sleifer, I.; Carignano, A. *Adv. Chem. Phys.* **1996**, *94*, 165.
(17) Sarmoira, C.; Blankschtein, D. *J. Phys. Chem.* **1992**, *96*, 1978.
(18) D'Arrigo, G.; Briganti, G. *Phys. Rev. E* **1998**, *58*, 713.
(19) Glatter, O., private comunication.
(20) See for example Prigogine, I.; Defay, R. *Chemical Thermodynamics*; Longmans Green: 1954.
(21) Lin, T. L.; Chen, S. H.; Roberts, M. F. *J. Am. Chem. Soc.* **1987**, *109*, 2321.
(22) Maisano, G.; Majolino, D.; Migliardo, P.; Venuto, S.; Aliotta, F.; Magazu, S. *Mol. Phys.* **1993**, *78*, 421.
(23) Bordi, F.; Cametti, C.; Di Biasio, A. *J. Phys. Chem.* **1988**, *92*, 4772.
(24) Degiorgio, V. *Nonionic Micelles*, International School of Physics, "Enrico Fermi" XC Course.
(25) Franks, F. *Water: a Comprehensive Treatise*; Vol. II, pp 463−464.
(26) Lunkenheimer, K.; Holzbaner, H. R.; Hirte, R. *Prog. Colloid Polym. Sci.* **1994**, *97*, 116.
(27) Priester, T.; Bartoszek, M.; Lunkenheimer, K. *J. Colloid Interface Sci.* **1998**, *208*, 6.
(28) Szleifer, I.; Ben-Shaul, A.; Gelbart, W. M. *J. Chem. Phys.* **1986**, *85*, 5345.
(29) Gruen, D. W. *J. Phys Chem.* **1985**, *89*, 146.
(30) Briganti, G.; Bonincontro, A. J. *Non-Cryst. Solids* **1998**, *235*, 704.